

Characteristics of screw-shaped ultrasonic motor that incorporates three transducers

Atsuyuki Suzuki (1), Kentaro Izumi (1) and Jiromaru Tsujino (2)

(1) Tokuyama college of technology, Shunan, Japan
(2) Kanagawa university, Yokohama, Japan

PACS: 43.35.Yb

ABSTRACT

We devised a screw-shaped ultrasonic motor that incorporates three separate transducers. Three bolt-clamped Langevin-type longitudinal vibration transducers (BLTs) were installed in the shape of a screw in order to generate torque. It is difficult for practical traveling-wave-type ultrasonic motors to generate higher torque because they are fragile. In order to realize a higher-torque ultrasonic motor, a transducer with high strength and large amplitude is required. A BLT satisfies this requirement. Vibration distributions were measured. The resonant frequency of the motor matched that of the BLT. The load characteristics of the motor were also measured. The maximum torque, revolution speed, and efficiency of the ultrasonic motor were 0.67 Nm, 582 rpm, and 7.63%, respectively. In addition, the transient response of the motor was measured. The motor attained stationary revolution within 1.5 ms and came to rest within 0.5 ms.

INTRODUCTION

Ultrasonic motors have unique characteristics such as high torque at low speed, high holding torque, silent motion, absence of magnetic noise, and freedom from external magnetic influence; these characteristics make them superior to conventional electric motors. Therefore, ultrasonic motors are expected to find widespread applications. However, their applications are limited to certain mechanisms, e.g., autofocus mechanisms of cameras.

One of the reasons why ultrasonic motors have not been widely utilized is that higher-torque ultrasonic motors have not yet been realized. Limitations of ultrasonic motors strongly depend on the limitations of piezoelectric elements. A piezoelectric element is resistant to compression stress but is vulnerable to tensile stress. If a practically used ultrasonic motor is driven under vibrations with large amplitudes, the piezoelectric elements would be damaged by tensile stress. In a bolt-clamped Langevin-type longitudinal vibration transducer (BLT), tensile failure is prevented by the application of a compressive prestress applied with a bolt. A BLT is a common source of vibration in high-power ultrasonic applications, and it features high strength and large amplitude.

However, when a BLT was used for an ultrasonic motor, the driving surface of the motor often wore down rapidly owing to repeated collisions with the rotor. Mitigating this problem can lead to wider applications of high-torque ultrasonic motors incorporated with BLTs. Two methods have been reported to improve the motor characteristics by reducing the wear in the driving surface of the motor: (1) the application of a driving method using a lubricant^[1] and (2) pressure controlling using an external vibration^[2].

In order to develop a high-torque motor, we devised a standing-wave-type ultrasonic motor that incorporates BLTs. Three BLTs are installed in the shape of a screw in order to generate torque. We had previously devised a screw-shaped ultrasonic motor that incorporates BLTs and a BLT connector^[3]. However, the driving frequency of the motor did not match the resonant frequency of the BLT. Therefore, the motor did not generate sufficient power.

In this study, we devised a new screw-shaped ultrasonic motor with better torque and measured its vibration and driving characteristics. The ultrasonic motor will find increased applications if its torque is enhanced. Such motors could then be used in high-torque applications such as robotic arms and door-opening systems intended for use in case of an earthquake.

CONFIGURATION

We had previously devised a one-piece-type screw-shaped ultrasonic motor that incorporated three BLTs and a BLT connector (Figure 1). Three BLTs (15 mm in diameter) were attached to the BLT connector. The BLT connector was made of an aluminum alloy (JIS A5052). This configuration had a flaw in that the driving frequency of the motor was not synchronous with the resonant frequency of the BLTs. Therefore, the motor did not generate sufficient power. This lack of synchronization of the driving frequency with the resonant frequency of the BLTs may have been due to the fact that the motor did not have free ends that were parallel to the emitting parts of the BLTs. Furthermore, the piezoelectric elements may not have been appropriately placed.

In this study, we devised a new screw-shaped ultrasonic motor that incorporates three separate transducers. The trans-

ducer consists of a BLT (diameter: 15 mm) and a stepped horn (vibration velocity transform ratio $N=2$). Figure 2 shows a photograph of the new screw-shaped ultrasonic motor, and Figure 3 shows the Elements of this motor. The motor has free ends that are parallel to the emitting parts of the BLTs. Therefore, it is easy to synchronize the driving frequency of the motor with the resonant frequency of the BLTs. Furthermore, stepped horns (JIS A2017) are installed in the motor to increase the vibration amplitude.

Three BLTs are installed in the shape of a screw to generate torque. The resonant frequency of the BLTs is 60 kHz. A cylindrical rotor is installed under static pressure by using a center rod and coil spring that function as the pressure sources. The rotor is made of steel (S45C) and is statically pressed against the driving surface using the pressure source. The rotor is 40 mm in diameter and 20 mm in thickness. The three BLTs are connected in a parallel configuration to an SIT power amplifier and all BLTs are driven in the same vibration phase. Furthermore, to extend the life of the motor, the driving surface of the motor was not composed of frictional material. The metal rotor part is driven directly by the driving surface of the metal stator. The connecting surfaces of the components were lapped by loose abrasives (#1000 polishing powder).

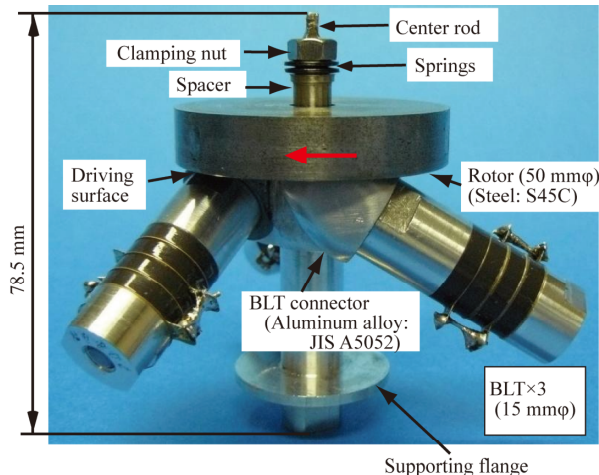


Figure 1. Configuration of a one-piece-type screw-shaped ultrasonic motor that incorporates three bolt-clamped Langevin type longitudinal vibration transducers (BLTs)

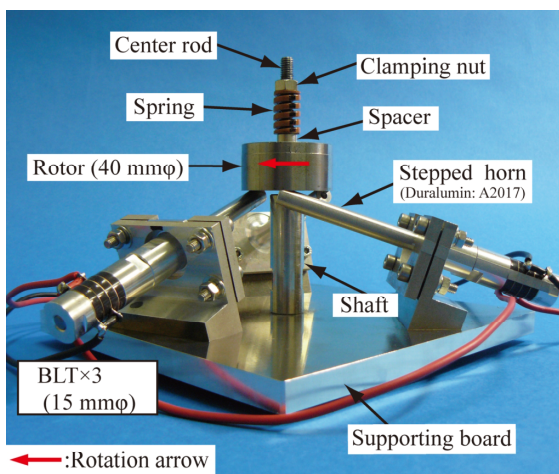


Figure 2. Configuration of a separate-type screw-shaped ultrasonic motor that incorporates BLTs.

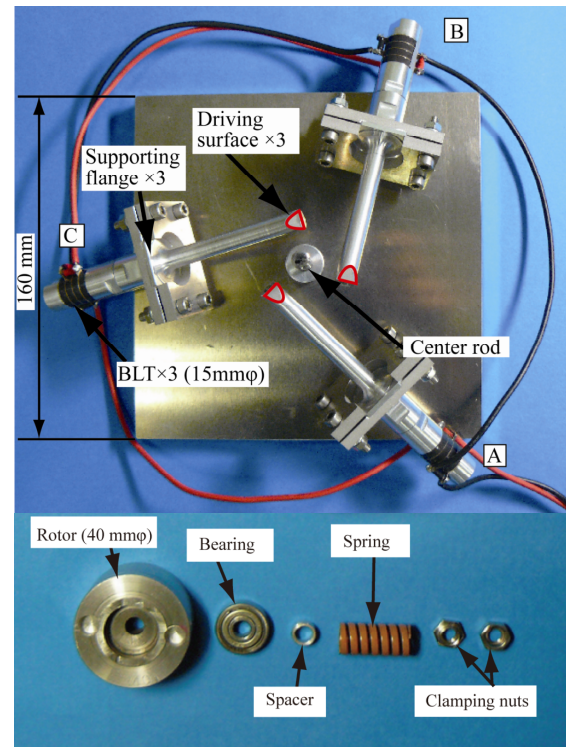


Figure 3. Elements of the separate-type screw-shaped ultrasonic motor.

VIBRATION CHARACTERISTICS

Admittance loops, vibration distributions, and vibration loci were measured. The admittance loops were measured using an impedance analyzer and the vibration distributions and loci were measured using a laser Doppler vibrometer. The three BLTs were driven simultaneously. The driving voltage was kept constant at 20 V (rms).

Admittance loops of the ultrasonic motor

Figure 4 shows the admittance loops of the separate-type ultrasonic motor, i.e., the ultrasonic motor comprising three separate bolt-clamped Langevin-type transducers (BLTs), with and without a rotor. When the rotor was installed, the resonant frequency of the BLTs changed from 60.01 kHz to 60.78 kHz. Furthermore, both the motional admittance $|Y_{m0}|$ and the quality factor decreased.

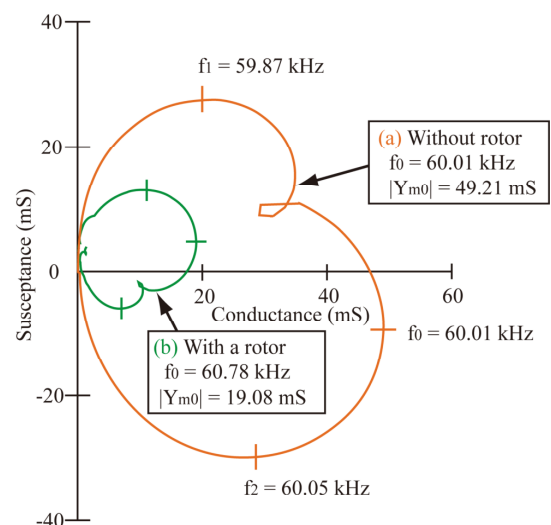


Figure 4. Admittance loops of the separate-type ultrasonic motor (a) without and (b) with a rotor.

Radial vibration distribution along the transducers

The radial vibration distribution along the transducers of the one-piece-type motor that we had previously devised is shown in Figure 5. Even though the resonant frequency of each BLT is around 60 kHz, the motor rotated at a frequency of 47.2 kHz. Hence, the vibration distribution was measured at the frequency of 47.2 kHz. An antinode exists in the standing wave along the free end of each BLT; this indicates that a bending vibration occurs along the BLT. We have designed the ultrasonic motor to operate in a longitudinal vibration mode, whereas the measured mode was a bending vibration mode.

The radial vibration distributions along transducers A, B, and C of the separate-type motor are shown in Figure 6. The motor rotated at a frequency of 59.1 kHz, and the vibration distributions were measured at this frequency, which is synchronous with the resonant frequency of the BLTs. The amplitude of transducer A was relatively larger. A node exists in the standing wave along the free end of transducer A; this result indicates that a longitudinal vibration occurs along the transducer A. However, nodes are separate slightly from free end for transducers B and C.

Relationship between driving voltage and vibration amplitude

The relationship between the driving voltage and the vibration amplitude at the free ends of the stepped horns is shown in Figure 7. The amplitude increases approximately linearly up to 100Vrms. The amplitudes of transducers B and C were similar, whereas the amplitude of transducer A was relatively smaller.

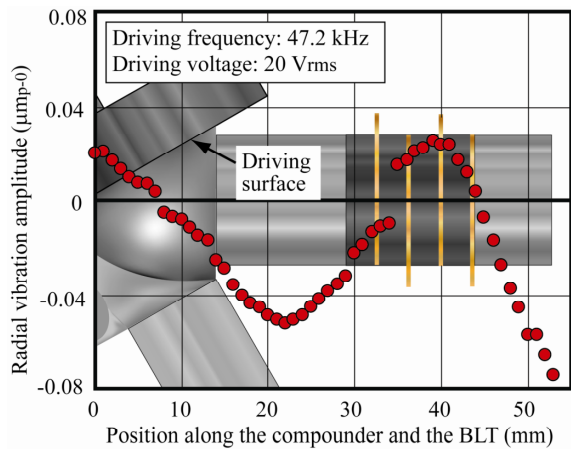


Figure 5. Radial vibration amplitude distribution along the transducer of the one-piece-type ultrasonic motor.

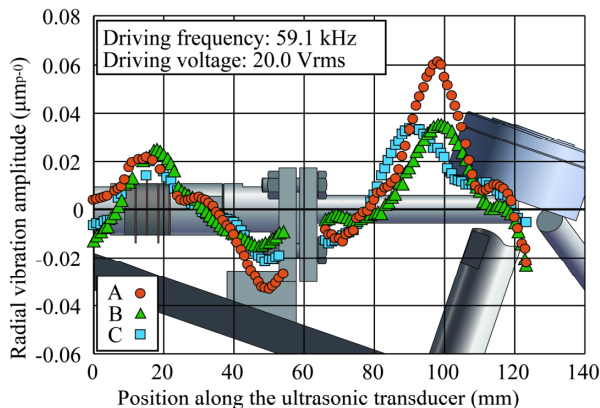


Figure 6. Radial vibration amplitude distributions along the ultrasonic transducers.

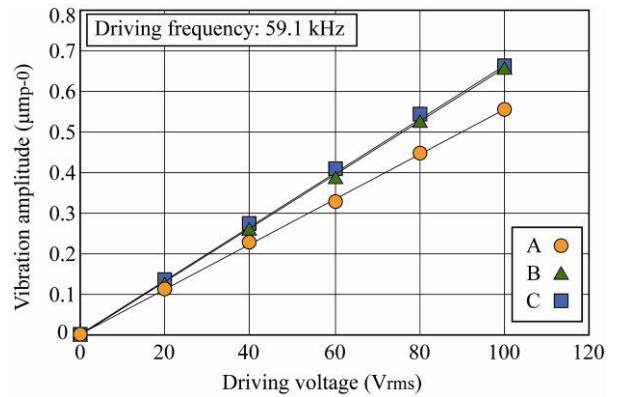


Figure 7. Relationship between driving voltage and vibration amplitude at the free ends of the transducers at no load condition.

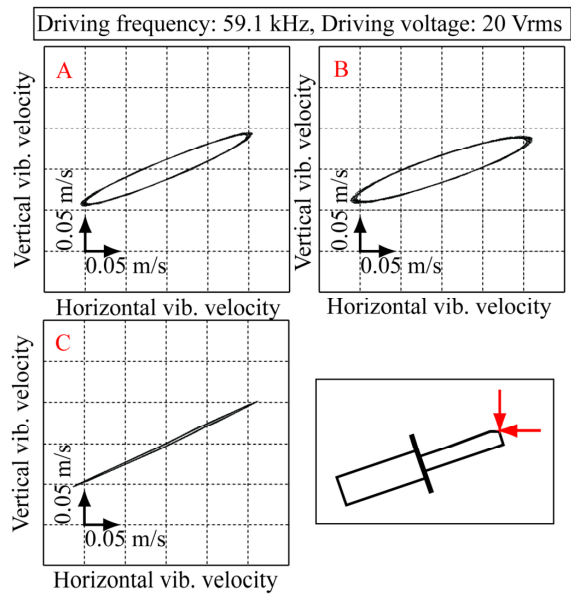


Figure 8. Vibration loci of the screw-shaped ultrasonic motor at no load condition.

Vibration loci

Vibration loci were observed at the driving surfaces of the transducers A, B, and C of the separate-type motor without a rotor (Figure 8). The loci of the transducers A and B were similar and elliptical, while the locus of transducer C was almost linear. It is desirable that the vibration loci at all driving surfaces be similar. All the driving surfaces were vibrated along both the horizontal and the vertical directions. This result indicates that a screw-shaped structure is conducive to generate torque.

DRIVING CHARACTERISTICS

Load characteristics

The load characteristics of the ultrasonic motors were measured by altering the load torque with the help of a powder brake. Torque and revolution speed were measured using a torque meter and a rotation meter, respectively. The input power was measured by a power meter using an electric current probe and a current-voltage multiplier. Furthermore, the mechanical output power of the motor was calculated from the torque and the revolution speed measured for various load torques.

The load characteristics of the one-piece-type motor are shown in Figure 9. This graph shows the relationships among the torque, revolution speed, electric input power, mechanical output power, and efficiency of the motor. The maximum torque, revolution speed, and efficiency of this motor are 0.41 Nm, 104 rpm, and 0.55% (at 0.21Nm), respectively, at a driving frequency of 48.1 kHz.

The load characteristics of the separate-type motor are shown in Figure 10. The maximum torque, revolution speed, and efficiency of this motor were 0.67 Nm, 582 rpm, and 7.63% (at 0.43Nm), respectively. All values were higher as compared to those of the one-piece-type motor. Table 1 summarizes the results of the load characteristics.

Transient response

The transient response of the screw-shaped ultrasonic motor that we devised is shown in Figure 11. The motor attained stationary revolution within 1.5 ms and came to rest within 0.5 ms. The revolution fluctuated slightly at stationary speed.

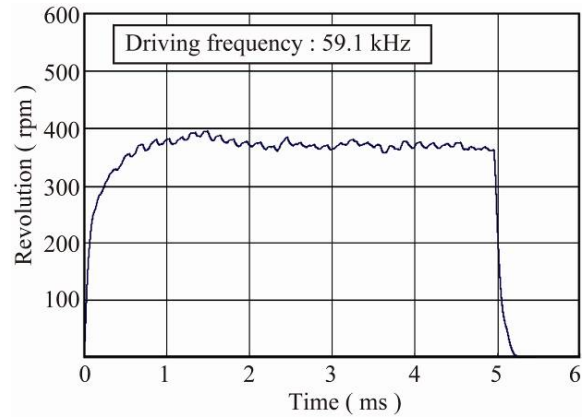


Figure 11. Transient response of the screw-shaped ultrasonic motor that incorporates stepped horns.

CONCLUSION

In this study, we devised a separate-type screw-shaped ultrasonic motor in order to meet the requirement of a high-torque motor. This motor incorporates BLTs and stepped horns; three BLTs were installed in the shape of a screw to generate torque. The developed ultrasonic motor can find widespread applications if its torque is enhanced. We studied the vibration and load characteristics of the motor. The maximum torque, revolution speed, and efficiency of the motor, which were 0.67 Nm, 582 rpm, and 7.63%, respectively, are higher than the corresponding values of the previously devised one-piece-type motor, which were 0.41 Nm, 104 rpm, and 0.55%, respectively. The one-piece-type motor rotated at a frequency of 48.1 kHz, even though the resonant frequency of its BLTs was 60 kHz. In contrast, the separate-type motor moved at 59.1 kHz, which is approximately equal to the resonant frequency of its BLTs. However, the vibration characteristics of the transducers were not similar. This drawback can be overcome by enhancing the precision with which the transducers are fabricated, particularly in the tapping operations of the horns. At present, the screw-shaped ultrasonic motor cannot generate sufficient power to realize a practical high-torque actuator. However, the performance of the ultrasonic motor can be further enhanced by synchronizing the vibration distributions along all the transducers.

ACKNOWLEDGMENT

This work was supported by JSPS Grant-in-Aid for Scientific Research (20760176).

REFERENCES

- 1 T. Ishii, S. Maeno, K. Nakamura, and S. Ueha, "Efficiency improvement of the friction drive in the ultrasonic motor using lubricant," Ultrasonic Symposium, 2001 IEEE vol. 1, 521-524 (2001)
- 2 A.Suzuki, M. Kihara, Y. Katsumata, K. Ishii, and J. Tsujino, "Ultrasonic rotary motor using complex transducers and torsional vibration rods and multiple longitudinal vibration transducers," Japan Journal of Applied Physics. **44**, No6B, 4642-4646 (2005)
- 3 A.Suzuki, Y. Nakamura, T. Ueoka, and J. Tsujino, "Configuration of a Screw-shaped Ultrasonic Motor," Proceedings of 2008 IEEE International Ultrasonics Symposium, 150-153 (2008)
- 4 A.Suzuki, K. Izumi, and J. Tsujino, "Novel screw-shaped Ultrasonic Motor to obtain high torque," Proceedings of 2009 IEEE International Ultrasonics Symposium, 1054-1057 (2009)

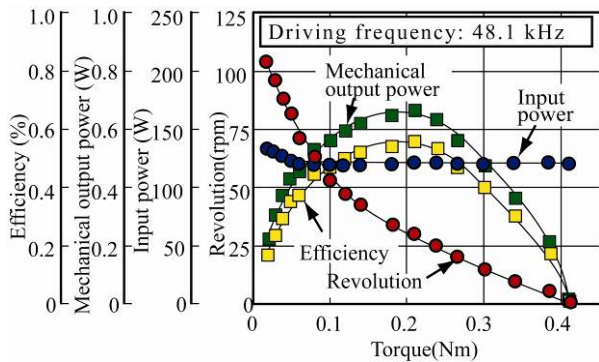


Figure 9. Load characteristics of the one-piece-type ultrasonic motor that incorporates three BLTs.

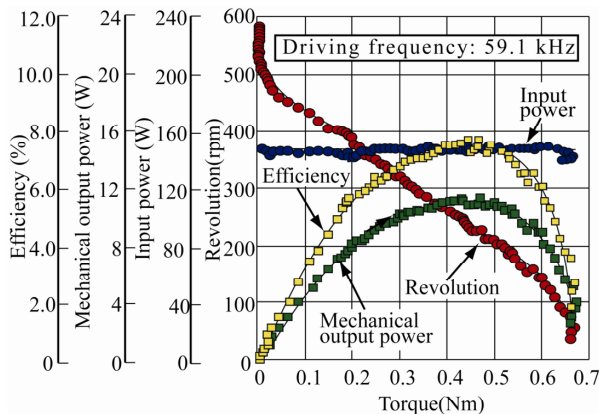


Figure 10. Load characteristics of the screw-shaped ultrasonic motor that incorporates stepped horns.

Table 1. Load characteristics of the screw-shaped ultrasonic motors that incorporate three BLTs.

	Max. torque	Max. revolution	Max. efficiency
<i>One-piece-type</i>	0.41	104	0.55
<i>Separate-type</i>	0.67	582	7.63